MOLECULAR AND CELLULAR BIOLOGY, July 2001, p. 4233–4245 Vol. 21, No. 13
0270-7306/01/$04.00+0 DOI: 10.1128/MCB.21.13.4233–4245.2001

New Function of *CDC13* in Positive Telomere Length Regulation

BETTINA MEIER, LUCIA DRILLER,† SIGRUN JAKLIN, AND HEIDI M. FELDMANN*

Institute for Biochemistry, University of Munich (LMU), D-81377 Munich, Germany

Received 26 February 2001/Returned for modification 28 March 2001/Accepted 13 April 2001

Two roles for the *Saccharomyces cerevisiae* Cdc13 protein at the telomere have previously been characterized: it recruits telomerase to the telomere and protects chromosome ends from degradation. In a synthetic lethality screen with *YKU70*, the 70-kDa subunit of the telomere-associated Yku heterodimer, we identified a new mutation in *CDC13, cdc13-4*, that points toward an additional regulatory function of *CDC13*. Although *CDC13* is an essential telomerase component in vivo, no replicative senescence can be observed in *cdc13-4* cells. Telomeres of *cdc13-4* mutants shorten for about 150 generations until they reach a stable level. Thus, in *cdc13-4* mutants, telomerase seems to be inhibited at normal telomere length but fully active at short telomeres. Furthermore, chromosome end structure remains protected in *cdc13-4* mutants. Progressive telomere shortening to a steady-state level has also been described for mutants of the positive telomere length regulator *TEL1*. Strikingly, *cdc13-4*/*tel1*Δ double mutants display shorter telomeres than either single mutant after 125 generations and a significant amplification of Y′ elements after 225 generations. Therefore *CDC13, TEL1*, and the Yku heterodimer seem to represent distinct pathways in telomere length maintenance. Whereas several *CDC13* mutants have been reported to display elongated telomeres indicating that Cdc13p functions in negative telomere length control, we report a new mutation leading to shortened and eventually stable telomeres. Therefore we discuss a key role of *CDC13* not only in telomerase recruitment but also in regulating telomerase access, which might be modulated by protein-protein interactions acting as inhibitors or activators of telomerase activity.

The ends of linear eukaryotic chromosomes form a special structure, the telomere. The telomeric DNA-protein complexes are essential for chromosome stability (49). They protect chromosomes from degradation and end-to-end fusion (54) and ensure their complete replication (41). In most eukaryotes, telomeric DNA contains a simple, repetitive sequence with the strand running toward the end of the chromosome being rich in G residues. For some organisms the configuration of the chromosome ends has been defined exactly. In hypotrichous ciliates the double-stranded region is followed by a 12- to 16-nucleotide-long single-stranded (ss) 3′ overhang (22, 24), whereas mouse and human chromosomes contain ss termini of 45 to 200 nucleotides (36, 39, 60). In the yeast *Saccharomyces cerevisiae* the telomere repeats consist of 300 ± 75 bp of $C_{1-3}A/TG_{1-3}$ DNA. Detectable ss extensions of the G-rich strand are generated at telomeres specifically during S phase in a telomerase-independent process (11, 57, 58). A specialized enzyme, telomerase, performs synthesis of telomeric DNA by extending the 3′ end of the G-rich strand of the telomere. Telomerase activity in *S. cerevisiae* depends on at least four protein subunits (encoded by *EST1, EST2, EST3*, and *CDC13*/*EST4*) (28, 34) and the RNA component (encoded by *TLC1*) (52). All subunits are essential for telomerase function in vivo, although only the catalytic subunit *EST2* and the RNA template *TLC1* are necessary for in vitro activity (6, 8, 30). Deletion of most individual components of the telomerase complex leads to inactivation of telomerase and thereby to a decrease in telomere length and to replicative senescence (28, 34).

However, deletion of *CDC13*/*EST4* leads to immediate cell cycle arrest and cell death (56). This phenotype is triggered by the accumulation of telomeric single-stranded DNA (ssDNA) that activates an *RAD9*-dependent G_2 arrest (16). Therefore Cdc13p was proposed to provide protection of the telomere from nucleolytic degradation by DNA end binding. This role is consistent with the finding that Cdc13p binds ss telomeric DNA in vitro (29, 40) and binds exclusively to telomeric, but not to internal, $C_{1-3}A/TG_{1-3}$ repeat sequences (5). Very recently the DNA binding domain of Cdc13p has been mapped to amino acids 557 to 694. Heterologous expression in *Escherichia coli* of a small, *CDC13*-derived polypeptide containing this region results in a protein that binds, like the full-length Cdc13p, with high affinity to ss telomeric DNA (23). A single amino acid missense mutation within this region of Cdc13p causes thermolabile DNA binding, and consistent with the presumption that Cdc13p DNA binding is essential to protect chromosome ends, this mutant is temperature sensitive for growth (23).

Besides its role in chromosome end protection, Cdc13p is involved in recruiting telomerase to telomeric DNA. *cdc13-2*^{est} mutant cells exhibit a senescence phenotype but can be rescued by expression of a Cdc13-2^{est}–Est1 fusion protein (12). These data suggest that Cdc13p is essential for loading telomerase to the telomere and that this process is mediated via interaction with Est1p. Interaction of Cdc13p and Est1p has

* Corresponding author. Mailing address: Institut für Biochemie der Universität München (LMU), Feodor-Lynen-Str. 25, D-81377 Munich, Germany. Phone: 49-89-2180 6962. Fax: 49-89-2180 6999. E-mail: fmann@lmb.uni-muenchen.de.

† Present address: Adolf-Butenandt-Institute for Cell Biology, University of Munich (LMU), D-80336 Munich, Germany.

been shown by two-hybrid criteria. Additionally, hemagglutinin (HA)-tagged Cdc13p can be copurified with a glutathione *S*-transferase (GST)–Est1 fusion protein from yeast extracts if both proteins were overexpressed (45). Furthermore, Cdc13p seems to be involved in the accurate regulation of telomerase recruitment, as several *CDC13* mutations, not yet mapped at the genomic level, confer either elongated telomeres (41, 18) or shortened telomeres (18).

In *S. cerevisiae* the steady-state level of telomeric GT repeat tract length seems to result from a balance between telomere elongation and telomere shortening (37). Many proteins involved in telomere length maintenance have been identified already. A major factor involved in negative telomere length regulation is the Rap1 protein, which binds with high affinity to specific sequences within the telomeric GT repeat tracts (7). Unregulated telomere elongation is prevented mainly by Rap1p and its interacting partners Rif1p and Rif2p (21, 31, 59). It has been proposed that a negative feedback mechanism determines the exact number of Rap1p molecules bound to telomeric DNA and regulates telomerase activity (37, 38). Recently, a model has been suggested in which a special folded structure prevents telomere elongation (46). In this model, the formation of the folded structure of the chromosome end depends on the length of the GT repeat tract and on the number of bound Rap1p.

At least two pathways are involved in positive telomere length control in *S. cerevisiae*. One pathway involves Tel1p and the Mre11-Rad50-Xrs2 complex, and disruption of any of these genes results in stable shortened telomeres (47). A second pathway affecting positive telomere length regulation involves the Yku heterodimer, which is also an essential component of the nonhomologous end-joining pathway (2–4, 44). As shown by in vivo cross-linking experiments, Ykup binds directly to telomeric DNA (19). Yku mutant strains display short but stable telomeres, and the ss telomeric overhang of the G-rich strand, usually restricted to S phase in wild-type cells, is present in Yku$^-$ cells throughout the entire cell cycle (19).

Using a genetic approach we identified a new mutation in *CDC13*, designated *cdc13-4*, that is lethal in combination with a deletion of either subunit of the Yku heterodimer. The telomeres of *cdc13-4* mutants shorten continuously for about 150 generations before eventually reaching a stable level comparable to the telomere length seen in Yku$^-$ mutants. *cdc13-4* causes no senescence phenotype, and a *cdc13-4*/*rad52* double mutant is viable for at least several hundred generations. A *cdc13-4*/*tel1*Δ double mutant displays enhanced telomere shortening compared to either single mutant and Y′ element amplification after 225 generations of growth. Coimmunoprecipitations reveal that HA_3-Cdc13-4p still associates with GST-Est1p when both proteins are overexpressed. In addition, in a *cdc13*Δ strain a Cdc13-4–Est1 fusion protein does not induce telomere elongation to the same extent as a wild-type Cdc13-Est1 fusion. The terminal chromosome configuration of *cdc13-4* mutants seems, besides the telomere shortening, unchanged, since no ss G-rich overhang can be detected by native in-gel hybridization. Our data indicate that Cdc13p functions in telomere length regulation independent of its roles in chromosome end protection and telomerase recruitment.

MATERIALS AND METHODS

***S. cerevisiae* strains, media, growth conditions, and transformation.** The strains used in this study are listed in Table 1. Cells were grown at 30°C using yeast extract-peptone-dextrose (YPD), yeast extract-peptone-galactose, or selective media as described elsewhere (14). Screening for synthetic lethal mutations was performed on YPD plates (9). For counterselection plates, 5-fluoroorotic acid (5-FOA) (bts) was added to selective media at a concentration of 1 mg/ml as described previously (9). To examine telomere length and the senescence phenotypes of strains over many generations, colonies derived from freshly germinated spores were streaked on YPD plates. After 48 h of incubation at 30°C, single colonies were restreaked on fresh YPD plates. This procedure was repeated up to nine times. Single colonies from different generations were then used for overnight inoculation and treated for DNA preparation. Yeast transformation was performed by the lithium acetate method (50).

Plasmids. The plasmid pCH-YKU70 used for the synthetic lethality screen was constructed as follows: a *Xho*I/*Eco*RI fragment containing a functional *YKU70* gene was isolated from the plasmid pRS316-YKU70 (15) and blunted with Klenow enzyme. This fragment was then cloned into pCH1122 (26) linearized with *Sma*I. Expression of Yku70p from pCH-YKU70 was verified by complementation of the temperature sensitive phenotype of a *yku70*-deficient strain and by reconstitution of Yku heterodimer DNA binding activity in a gel retardation assay (15). The *CDC13* expression plasmid pRS314-CDC13 was generated as follows: a 4.7-kb *Apa*I fragment containing 712 bp 5′ of the start codon, the entire open reading frame (ORF) of *CDC13*, and 1,200 bp 3′ of the stop codon was isolated from the library plasmid GP2a. This fragment was ligated to pRS314 (51), linearized with *Kpn*I/*Sac*I, and blunted with Klenow enzyme. To generate the plasmid pRS314-cdc13-4 expressing the mutated *CDC13* allele, a 900-bp DNA fragment was amplified by PCR from genomic DNA of mutant LDM29 by using the primers CDC13-ATG (5′-ACG TGT CGA CCC GGG ATG GAT ACC TAG AAG AGC CTG AG-3′) and CDC13-900 (5′-GAA ATA TTT CCC GGT AGA GGA GG-3′). The PCR product was subcloned into pZErO-2 (Invitrogen) and sequenced. A *Xho*I/*Nsi*I fragment carrying the *cdc13-4* point mutation was then excised from pZ-cdc13-4 and ligated to the vector pRS314-CDC13 digested with *Xho*I/*Nsi*I. To generate several *CDC13* disruption constructs, pRS314-CDC13 was digested with *Xho*I/*Aat*II, thereby deleting the entire ORF of *CDC13* except 57 bp at the 5′ end. This fragment was replaced by a marker cassette of either KanMX4 or *URA3*, resulting in plasmid p-cdc13Δ::KanMX4 or p-cdc13Δ::URA3, respectively. The plasmid pRS-cdc13-4-KanMX4 was generated for genomic integration of the *cdc13-4* allele by linearizing pRS314-cdc13-4 with *Aat*II, blunting it with Klenow enzyme, and inserting the KanMX4 marker cassette.

To generate *CDC13-EST1* and *cdc13-4–EST1* fusion constructs, the *EST1* gene was amplified from genomic DNA from strain W303a using primers Est1*Sac*I (forward: 5′-GAG CTC ATG GAT AAT GAA GAA GTT AAC G-3′) and Est1*Sal*I*Sma*I (reverse: 5′-GTC GAC CCC GGG TCA AGT AGG AGT ATC TGG CAC-3′). A C-terminal fragment of *CDC13* was amplified using primers Cdc13-P3 (5′-CTG GTG CCA GGC GTC AAT TGC-3′) and Cdc13-P4Sma (5′-ATC CCG GGC GAG GTG GGA ACG GCT CCG-3′) and cloned into plasmid pZErO-2. The *EST1* fragment was digested using *Sma*I/*Hpa*I and ligated into pZ-CDC13-P3P4Sma linearized with *Sma*I. The correct orientation of the construct was verified by restriction analysis. The plasmid was then cut with *Sac*II/*Pst*I, and the DNA fragment containing C-terminal *CDC13-EST1* was isolated. pRS314-CDC13 was digested with *Sac*II/*Not*I, and a 3.1-kb fragment containing the N-terminal part of *CDC13* and the *CDC13* promoter was isolated. Both fragments were then ligated to pRS314 *Not*I/*Pst*I, resulting in pRS314-CDC13-EST1. To delete the *Hin*dIII vector site, pRS314-CDC13-EST1 was cut with *Pst*I/*Apa*I, treated with T4 polymerase, and religated. The religated vector was cut with *Not*I/*Kpn*I, and the *CDC13-EST1* fragment was isolated and ligated to pRS316 *Not*I/*Kpn*I to obtain pRS316-CDC13-EST1. The plasmid pRS316-cdc13-4-EST1 was generated by restriction of pRS316-CDC13-EST1 with *Hin*dIII and replacing the resulting internal *CDC13 Hin*dIII fragment by the corresponding *cdc13-4 Hin*dIII fragment. The correct orientation of the *cdc13-4 Hin*dIII fragment was checked by restriction analysis, and sequencing confirmed the single base pair exchange in pRS316-cdc13-4-EST1.

Gene disruption. The *yku70*-deficient strain KαL7 was generated by disruption of the *YKU70* gene in K2348α as described previously (15). Gene disruption was verified by Southern blot analysis. To disrupt the *CDC13* gene, plasmids pRS314-cdc13Δ::URA3 and pRS-cdc13Δ::KanMX4 were digested with *Apa*LI and *Kpn*I, and the resulting linear disruption construct was used to transform several diploid strains to Ura$^+$ or G418 resistance (Table 1). Disruption of the *CDC13* gene was verified by Southern blot analysis. The yeast strain BMY13 carrying a genomic integrated *cdc13-4* allele was generated by transforming

TABLE 1. Yeast strains used in this study[a]

Strain	Genotype(s)	Reference
K2348α	*matα ade2-1 ade3 trp1-1 can1-100 leu2-3,112 his3-11,15 ura3 Gal*$^+$ *psi*$^+$	17
KαL7	K2348α *yku70*::*LEU2*	This study
CEN.PK2aα	*mat**a**/α ura3-52/ura3-52 his3-Δ1/his3-Δ1 leu2-3,112/leu2-3,112 trp1-289/trp1-289 MAL2-8*^{c}*/MAL2-8*^{c} *SUC2/SUC2*	1
LDY05	CEN.PK2aα *yku70*::*URA3*/*yku70*::*LEU2*	This study
LDY06	CEN.PK2aα *yku80*::*kanMX4*/*yku80*::*kanMX4*	This study
LDY54	LDY05 *cdc13*::*kanMX4*/*CDC13*	This study
LDY55	LDY06 *cdc13*::*URA3*/*CDC13*	This study
W303aα	*mat**a**/α leu2-3,112/leu2-3,112 ura3-1/ura3-1 his3-11,15/his3-11,15 trp1-1/trp1-1 ade2-1/ade2-1 can1-100/can1-100 rad5-535*	15
WaUαL	W303aα *yku70*::*URA3*/*yku70*::*LEU2*	15
LDY50	W303aα *cdc13*::*URA3*/*CDC13*	This study
LDY46	WaUαL *cdc13*::*kanMX4*/*CDC13*	This study
LDY53	W303 *cdc13*::*URA3* + pRS314-cdc13-4	This study
BMY13	W303aα *cdc13*::*URA3*/*cdc13-4*::*kanMX4*	This study
BMY14	W303aα *cdc13*::*URA3*/*cdc13-4*::*kanMX4 rad52*Δ::*His3MX6*/*RAD52*	This study
BMY17	W303a *cdc13-4*::*kanMX4*	This study
BMY18	W303 *cdc13-4*::*kanMX4 rad52*Δ::*His3MX6*	This study
BMY56	W303aα *cdc13-4*::*kanMX4*/*CDC13*	This study
BMY57	W303aα *cdc13-4*::*kanMX4*/*CDC13 tel1*Δ::*His3MX6*/*TEL1*	This study
BMY58	W303aα *cdc13-4*::*kanMX4*/*CDC13 est2*Δ::*TRP1*/*EST2*	This study
BMY59-6A	W303a wt spore derived from BMY58	This study
BMY59-6B	W303α *cdc13-4*::*kanMX4* derived from BMY58	This study
BMY59-6C	W303a *est2*Δ::*TRP1* derived from BMY58	This study
BMY59-6D	W303α *cdc13-4*::*kanMX4 est2*Δ::*TRP1* derived from BMY58	This study
BMY60-11F	W303α *tel1*Δ::*His3MX6* spore derived from BMY57	This study
BMY60-11G	W303a *cdc13-4*::*kanMX4* derived from BMY57	This study
BMY60-11H	W303α *cdc13-4*::*kanMX4 tel1*Δ::*His3MX6* derived from BMY57	This study
BMY60-11I	W303a wt derived from BMY57	This study
BMY62	W303aα *CDC13*/*cdc13*Δ::*kanMX4*	This study
BMY64	W303 hap *cdc13*Δ::*kanMX4* + pRS316-CDC13-EST1	This study
BMY65	W303 hap *cdc13*Δ::*kanMX4* + pRS316-cdc13-4-EST1	This study
HFY80	W303aα *HIS3MX6-GAL1*-HA$_3$::*CDC13*/*CDC13*	
HFY81	W303aα *TRP1-GAL1-GST*::*EST1*/*EST1*	This study
HFY81-8A	W303 hap *TRP1-GAL1-GST*::*EST1* derived from HFY81	This study
HFY82	W303aα *HIS3MX6-GAL1*-HA$_3$::*CDC13*/*CDC13 TRP1-GAL1-GST*::*EST1*/*EST1* derived from HFY81	This study
HFY82-6B	W303 hap *HIS3MX6-GAL1*-HA$_3$::*CDC13* derived from HFY82	This study
HFY82-4C	W303 hap *HIS3MX6-GAL1*-HA$_3$::*CDC13 TRP1-GAL1-GST*::*EST1*	This study
HFY84	W303aα *HIS3MX6-GAL1*-HA$_3$::*cdc13-4*/*CDC13* derived from BMY56	This study
HFY86	W303aα *HIS3MX6-GAL1*-HA$_3$::*cdc13-4*/*CDC13 TRP1-GAL1-GST*::*EST1*/*EST1* derived from HFY84	This study
HFY86-3A	W303 hap *HIS3MX6-GAL1*-HA$_3$::*cdc13-4 TRP1-GAL1-GST*::*EST1* derived from HFY86	This study
HFY86-9D	W303 hap *HIS3MX6-GAL1*-HA$_3$::*cdc13-4 TRP1-GAL1-GST*::*EST1* derived from HFY86	This study

[a] wt, wild type; hap, haploid.

LDY50 using the *Apa*I/*Kpn*I fragment excised from pRS-cdc13-4-KanMX4. The transformed cells were plated on synthetic-dextrose minimal plates lacking uracil and containing 200 mg of G418/liter. Colonies arising from these plates were screened by PCR for correct integration of the marker gene. To verify the integration of the *cdc13-4* point mutation, a PCR fragment spanning the corresponding part of the *CDC13* gene was amplified and sequenced. BMY14 (W303aα *cdc13*::*URA3*/*cdc13-4*::*kanMX4 rad52*Δ::*His3MX6*/*RAD52*) was generated by replacement of the *RAD52* ORF in BMY13 by PCR-based gene disruption (55). Sporulation of BMY13 and BMY14 resulted in haploid spores carrying the *cdc13-4* point mutation (BMY17) and double mutant *cdc13-4*/*rad52*Δ (BMY18), respectively. Strain BMY56 was generated by crossing BMY17 with W303a. This strain was propagated for several generations and then used to introduce either a *tel1* or *est2* deletion. *TEL1* was deleted by PCR-based replacement of the entire ORF with a His3MX marker (BMY57), and the *EST2* gene was replaced by the *TRP1* selection marker (BMY58). Transformants arising after incubation on selective media were screened by PCR for integration of the disruption constructs. Both heterozygous strains were then sporulated, and tetratype tetrads BMY59 and BMY60 were used for growth studies and analysis of telomere length phenotypes. To analyze expression of Cdc13-Est1 fusion proteins in a *cdc13*Δ strain, BMY62 was transformed with pRS-CDC13-EST1 or pRS316-cdc13-4-EST1 and sporulated on plates lacking uracil. BMY64 and BMY65 were isolated after tetrad dissection of BMY62+pRS-CDC13-EST1 and BMY62+pRS-cdc13-4-EST1, respectively.

Induced expression of HA$_3$-*CDC13*, HA$_3$-*cdc13-4*, and GST-*EST1*. For induced overexpression of HA$_3$-tagged *CDC13* and *cdc13-4*, the *GAL1* promoter together with the HA$_3$ tag was introduced in front of the genomic copy of *CDC13* in W303aα or *cdc13-4* in BMY56. Integration of *GAL1*-HA$_3$ was performed by PCR-based methods as described previously (32) using the HIS3MX6 marker for selection. Correct integration of the HIS3MX-*GAL1*-HA$_3$ construct in the resulting strains HFY80 (HA$_3$-*CDC13*) and HFY84 (HA$_3$-*cdc13-4*) was verified by analytic PCR and sequencing of the PCR product. Expression of HA$_3$-Cdc13p and HA$_3$-Cde13-4p was analyzed by Western blotting using monoclonal anti-HA antibody 9F10 (Roche). The same PCR-based strategy was used to generate strains expressing GST::Est1 fusion protein under control of the *GAL1* promoter. The *TRP1-GAL1*-GST construct was introduced in W303aα, HFY80, and HFY84 resulting in the strains HFY81 (GST::EST1/EST1), HFY82 (HA$_3$-*CDC13*/*CDC13* GST::*EST1*/*EST1*) and HFY86 (HA$_3$-*cdc13-4*/*CDC13* GST::*EST1*/*EST1*). Correct integration was verified by analytic PCR and sequencing of the PCR product. Expression of GST::Est1p was analyzed by Western blotting using monoclonal anti-GST antibody (Sigma). Strains were grown on yeast extract-peptone media containing 2% galactose for induced expression of HA$_3$-*CDC13*, HA$_3$-*cdc13-4*, and GST::*EST1*. Strains HFY81, HFY82, and HFY86 were sporulated to generate haploid strains expressing the tagged Cdc13 and/or Est1 proteins. Tetrad analysis was performed on yeast extract-peptone plates containing galactose to allow expression of HA$_3$-Cdc13p, HA$_3$-Cdc13-4, and GST::Est1p. Spores expressing the tagged proteins were identified by marker analysis, and the resulting strains

HFY81-8A (GST::*EST1*), HFY82-6B (HA_3-*CDC13*), HFY82-4C (HA_3-*CDC13* GST::*EST1*), HFY86-3A (HA_3-*cdc13-4* GST::*EST1*), and HYF86-9D (HA_3-*cdc13-4* GST::*EST1*) were verified by Western blotting.

Immunoprecipitation. Coimmunoprecipitation experiments to analyze the interaction of GST-Est1p-HA_3-Cdc13p and GST-Est1p-HA_3-Cdc13-4p were performed using strains HFY82-4C, HFY86-3A, HFY86-9D, and, as controls, HFY81-8A and HFY82-6B. Crude extracts were prepared as follows: yeast strains were grown overnight in YPGal, diluted to an optical density at 600 nm (OD_{600}) of 0.2, and grown to an OD_{600} of 0.8 to 1.2 in yeast extract-peptone-galactose. Cells were lysed in 20 mM Tris (pH 8.0)–200 mM NaCl–1 mM EDTA–1 mM dithiothreitol–0.01% NP-40–10% glycerol with one protease inhibitor cocktail tablet per 5 ml (complete, Mini, EDTA-free; Roche) in a bead beater. After centrifugation the soluble protein fraction was diluted 1:1 with lysis buffer containing 1% NP-40 and 0.2% Triton X-100. Crude extract (1,000 μg) was incubated with monoclonal anti-GST antibody, clone GST-2 (Sigma), for 1 h at 4°C, and then G-Sepharose (Pharmacia) was added. After incubation for 1 h at 4°C G-Sepharose beads were collected by centrifugation and washed twice with lysis buffer containing 0.5% NP-40–0.1% Triton X-100, twice with lysis buffer containing 1% NP-40–0.1% Triton X-100, and twice with lysis buffer containing 450 mM NaCl. The beads were treated with 1,000 U of DNase I/ml in lysis buffer containing 1 mM $MgCl_2$ and then washed twice with lysis buffer containing 450 mM NaCl and 350 mM potassium acetate. After 15 μl of Laemmli buffer was added, beads were heated 3 min at 95°C and the supernatant was loaded onto an 8% sodium dodecyl sulfate gel. Proteins were visualized by enhanced chemiluminescence Western blotting using anti-HA antibody 9F10 (Roche) and anti-GST antibody clone GST-2 (Sigma).

Synthetic lethality screen. Stationary phase cells of KαL7 carrying the plasmid pCH-YKU70 were mutagenized with 3% ethyl methanesulfonate (EMS) for 90 min resulting in 15.6% survival. After EMS treatment, cells were plated on YPD plates containing 4% glucose to facilitate development of the red pigment. Uniformly red colonies were colony purified three times. Those which remained stably red under nonselective conditions were tested for sensitivity to 5-FOA. To test whether 5-FOA-sensitive cells were dependent on *YKU70* expression rather than other components of the plasmid pCH-YKU70, the mutants were transformed with a second plasmid, pRS314-YKU70, expressing Yku70p and containing *TRP1* for selection. As a control, mutants were transformed with pRS314. Mutants carrying pRS314-YKU70 or pRS314 were retested for their ability to form red-white sectors and their growth on 5-FOA. Out of 20,520 mutagenized cells, five mutants were clearly dependent on *YKU70* expression. These mutants were stably red on YPD and sensitive to 5-FOA if transformed with the pRS314 vector control, but they displayed red-white sectoring colonies and growth on 5-FOA after transformation with pRS314-YKU70.

Complementation of *YKU70* dependence. The mutant LDM29 was transformed using a single-copy genomic yeast library (ATCC 77164) and plated on Trp^- media. Out of 12,500 primary transformants, 15 plasmids were isolated leading to red-white sectoring colonies even after retransformation. In addition, these 15 plasmids enabled LDM29 cells to grow on 5-FOA-containing media, indicating that those cells were independent of *YKU70* expression. Restriction analysis revealed the isolation of three different genomic fragments capable of complementing the dependence on *YKU70*. To identify the isolated fragments, the 5′ and 3′ ends of the fragments were sequenced using vector-specific primers.

Identification of the *cdc13-4* mutation. The genomic mutation in LDM29 was mapped by gap repair (42). Plasmid pRS314-CDC13 was digested using different combinations of restriction enzymes. The resulting linear plasmids were transformed into LDM29. Generation of a functional *CDC13* gene by gap repair results in cells independent of *YKU70* expression, therefore displaying a red-white sectoring phenotype. Only cells transformed with pRS314-CDC13 with a *Xho*I/*Nsi*I fragment spanning bp +57 to +830 of the *CDC13* coding sequence deleted did not display red-white sectoring colonies and were sensitive to 5-FOA, indicating that a plasmid carrying the mutated allele of *CDC13* was generated. To identify the mutation, a fragment corresponding to the mutated region in *CDC13* was amplified by PCR from genomic DNA of LDM29 and was sequenced.

Yeast DNA extraction and analysis of telomeric DNA. Genomic DNA was isolated from 5- to 7-ml overnight cultures using the nucleon MiY DNA extraction kit (Amersham Life Science). For analysis of telomere length, genomic DNA was digested overnight using *Xho*I and separated on a 1% agarose gel in 1× Tris-acetate-EDTA buffer. DNA was transferred to nylon membranes (HybondN$^+$) by vacuum blotting using 0.4 N NaOH. Detection of telomeric DNA fragments was performed as described elsewhere (2). Nondenaturing in-gel hybridization was performed as described previously (11).

RESULTS

Isolation of the *cdc13-4* mutant. Yku^- mutant cells are temperature sensitive for growth (14, 15). To investigate the essential role of the Yku heterodimer at 37°C, we performed a synthetic lethality screen to isolate mutants in which *YKU70* would be essential for viability. Therefore we disrupted the *YKU70* gene in K2348α and tested the resulting mutant KαL7 for phenotypes specific for Yku^- mutants. KαL7 is temperature sensitive for growth at 37°C, deficient in nonhomologous end joining, slightly sensitive to methyl methanesulfonate, and displays shortened telomeres (data not shown). The *YKU70* gene cloned into plasmid pCH1122 (pCH-YKU70) complemented the phenotypes of KαL7, indicating a functional expression of *YKU70* from the plasmid. KαL7-pCH-YKU70 colonies grown on YPD displayed a red-white sectoring phenotype, showing that pCH-YKU70 was not essential for growth at 30°C under nonselective conditions.

After EMS mutagenesis of KαL7-pCH-YKU70 we isolated five stably red mutants, which clearly required *YKU70* expression for viability (see Materials and Methods). To identify the mutated gene causing the requirement for *YKU70* expression we transformed one mutant, LDM29, with a single-copy yeast library and screened for sectoring colonies indicating that pCH-YKU70 was no longer essential for viability. Plasmids isolated from 15 sectoring colonies revealed three independent clones, two of them carrying a DNA fragment containing the full-length *YKU70* gene. The third plasmid, GP2a, contained a fragment of chromosome IV from YDL57269 to YDL68607. This fragment encoded five ORFs, among them YDL220c coding for *CDC13*/*EST4*.

Cdc13p, like the Yku heterodimer, has been shown to be an important factor for telomere maintenance. Therefore we subcloned the *CDC13* gene from plasmid GP2a into the single-copy vector pRS314 (51). After transformation with the resulting plasmid pRS314-CDC13, LDM29 displayed a clear sectoring phenotype indicating that a mutation in *CDC13* caused dependence on Yku70p expression (data not shown). Using the gap repair method (42) we identified a 773-bp fragment near the 5′ end of the *CDC13* gene carrying the mutation. Sequencing of this fragment revealed the presence of a single point mutation (at position 703, changing a cytosine to a thymine), thereby leading to the amino acid exchange proline 235 to serine (P235S). Since this mutation differs from the *CDC13* mutants already described in the literature, we designated it *cdc13-4*.

Synthetic lethality of *cdc13-4* with Yku. We isolated the *cdc13-4* mutation in a synthetic lethality screen with *YKU70*. To verify the synthetic lethal phenotype we reintroduced the *cdc13-4* mutation in the homozygous *yku70* strain WaLαU. Therefore we disrupted the *CDC13* gene in WaUαL and transformed the resulting strain LDY46, heterozygous for *CDC13*, with pRS-cdc13-4. As expected, we obtained only two colony-forming spores after sporulation and tetrad dissection of LDY46-pRS-cdc13-4 (data not shown). None of the viable spores was resistant to G418 (the KanMX marker gene was used for *CDC13* disruption), indicating that all viable spores contain the wild-type allele of *CDC13*. The nonviable spores were examined by microscopy. We found many of these spores germinated but arrested at a two-cell stage. In a very few cases we observed microcolonies containing up to 20 cells, which lysed

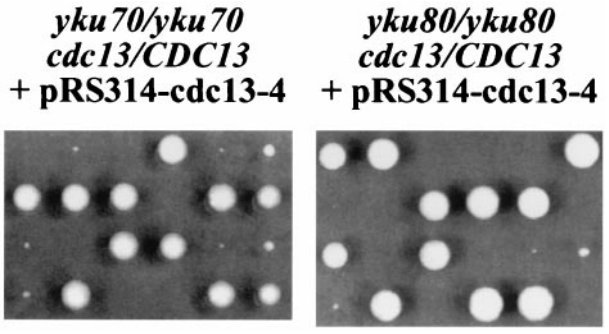

FIG. 1. Synthetic lethality of *cdc13-4* with the Yku heterodimer. Diploid strains CEN.PK2aα *yku70/yku70 cdc13/CDC13* and CEN.PK2aα *yku80/yku80 cdc13/CDC13* were transformed with plasmid pRS314-cdc13-4. Transformants were sporulated and tetrads were dissected using a Singer SMS Micromanipulator. Individual spores of each tetrad were placed down the columns on the YPD plates and incubated at 30°C for 3 to 4 days.

after 2 to 3 days of incubation at 30°C. To show that these phenotypes were not due to synthetic effects caused by the *RAD5* mutation in the W303 background (13), we repeated the experiment in a CEN.PK2 strain. In this case we examined the synthetic lethality of *cdc13-4* in a *yku70*- and a *yku80*-deficient CEN.PK2 strain, LDY54 and LDY55, respectively.

Again we found only two colony-forming spores for most of the dissected tetrads. In some cases one or two microcolonies arose (Fig. 1). Cells from these microcolonies were not viable after restreaking on YPD plates (data not shown). Our data show that *cdc13-4* is synthetic lethal with either *yku70* or *yku80* deletion. Therefore we suggest that a *cdc13-4* mutant is dependent on a functional Yku heterodimer.

Telomeres of *cdc13-4* mutants shorten to a steady-state level. To investigate the phenotype of a *cdc13-4* single mutant we generated a haploid strain expressing the mutated *CDC13* gene (LDY53). One allele of *CDC13* was deleted in W303aα, and the resulting heterozygous strain LDY50 was transformed using pRS314-cdc13-4. After sporulation and tetrad dissection, some tetrads were able to form three viable colonies (data not shown). Since disruption of *CDC13* is lethal, the tetrads resulting in three colony-forming spores should contain one spore carrying a disrupted *cdc13* allele and the plasmid expressing *cdc13-4*. All three tetrads tested formed two colonies unable to grow on uracil- or trytophan-lacking media and exhibited wild-type fragment size in a Southern blot. One colony was prototrophic for uracil and tryptophan and displayed a disrupted genomic *CDC13* allele and Southern blot signals corresponding to the plasmid pRS314-cdc13-4 (data not shown). This colony corresponds to the *cdc13-4* mutant LDY53.

One important role of Cdc13p in telomere maintenance is loading telomerase to its ss template at chromosome ends. In *cdc13-2*^{est} mutants the loading function is abolished, presumably by inhibition of the Cdc13p-Est1p interaction, thereby resulting in progressive telomere shortening and senescence (40). To investigate the effect of the *cdc13-4* mutation on telomere stability we performed long-term growth experiments using strain LDY53. No growth reduction was observed for the *cdc13-4* mutant for more than 250 generations (data not shown), suggesting that this mutation causes no senescence

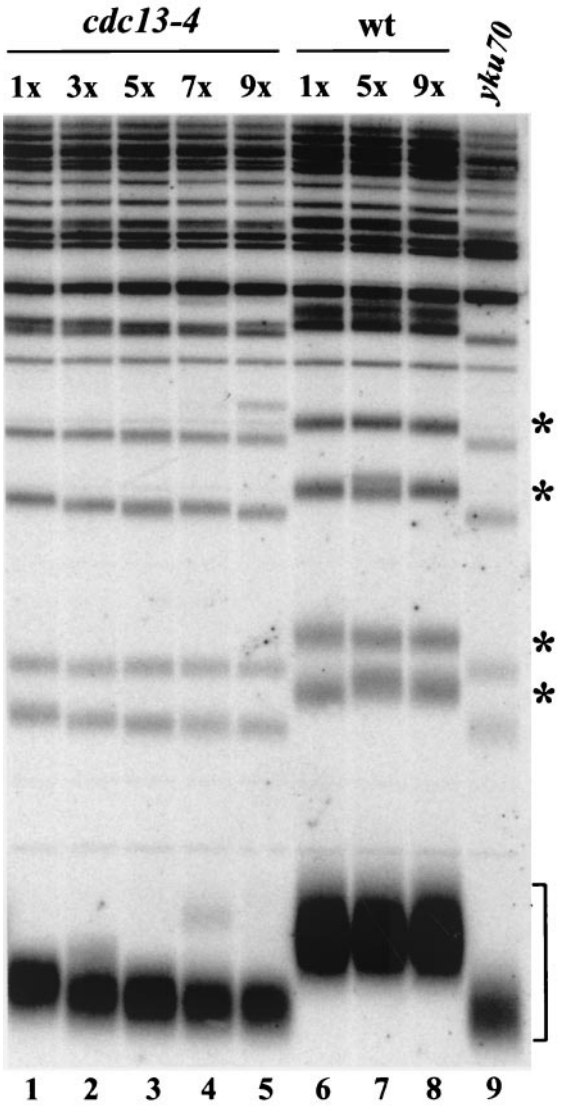

FIG. 2. Long-term analysis of the telomere length of a *cdc13-4* mutant. Southern blot of genomic yeast DNA, probed with a telomere-specific poly$(GT)_{20}$ oligonucleotide, is shown. The bracket indicates the telomeric GT repeat band derived from Y′ element-containing chromosomes. Asterisks indicate terminal fragments derived from non-Y′ element-containing chromosomes. W303 wild-type (wt) and W303 *cdc13*::*URA3* + pRS314-cdc13-4 strains from one tetrad were propagated on YPD for 250 generations. Therefore colonies derived from freshly germinated spores were streaked on YPD plates. After 48 h of incubation at 30°C, single colonies were restreaked on fresh YPD plates. Cells were estimated to have undergone 20 to 25 divisions per streakout. Numbering at the top of the lanes (1x, 3x, etc) indicates the number of times of restreaking. Single colonies from different generations were then used for overnight inoculation and treated for DNA preparation. Genomic DNA was prepared as described in Materials and Methods. Lane 1, *cdc13-4*, 50 generations; lane 2, *cdc13-4*, 100 generations; lane 3, *cdc13-4*, 150 generations; lane 4, *cdc13-4*, 200 generations; lane 5, *cdc13-4*, 250 generations; lane 6, W303 wt, 50 generations; lane 7, W303 wt, 150 generations; lane 8, W303 wt, 250 generations; and lane 9, W303a *yku70*.

phenotype. To better understand the effect of the *cdc13-4* mutation, we examined telomere length in this mutant after various generations (Fig. 2).

cdc13-4 cells displayed a significant shortening of the telo-

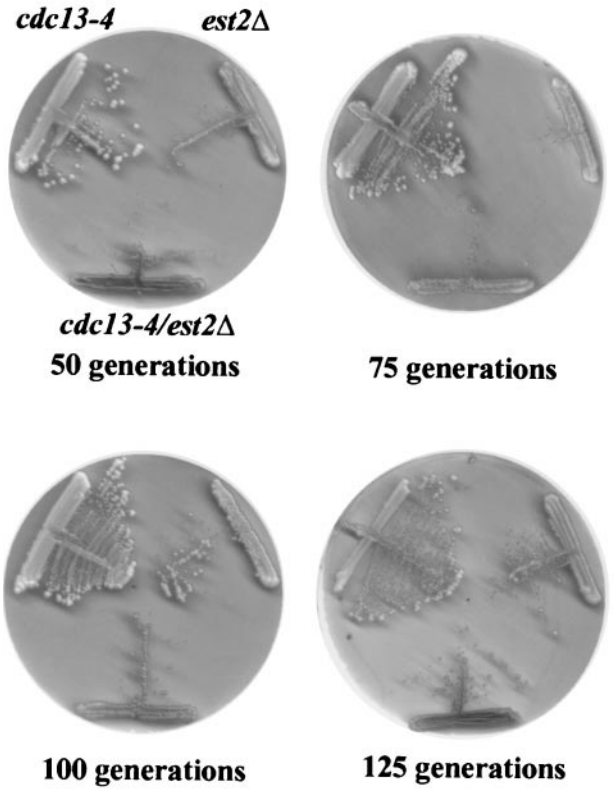

FIG. 3. Viability of *cdc13-4, est2*Δ, and *cdc13-4 est2*Δ strains. After sporulation, *cdc13-4, est2*Δ, and *cdc13-4*/*est2*Δ mutant cells from a single tetrad were successively streaked on YPD plates to test senescence.

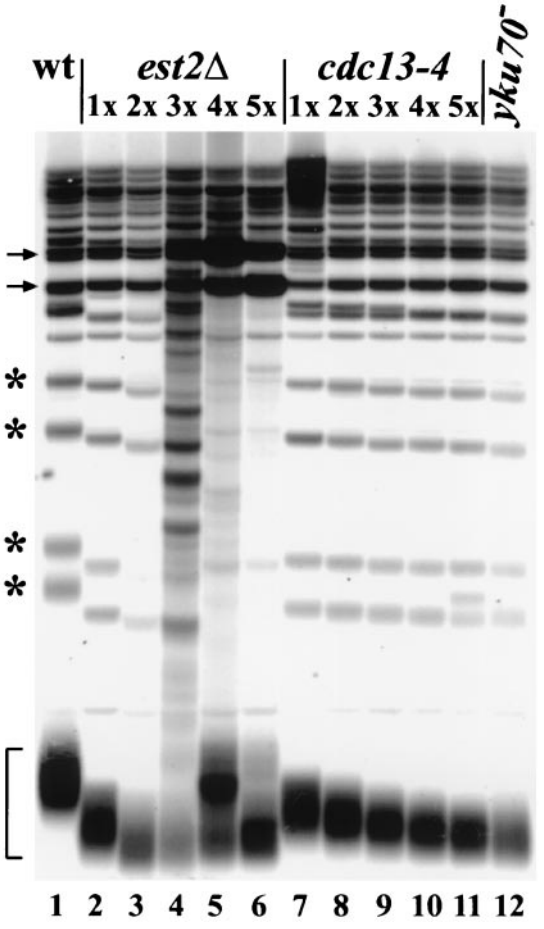

FIG. 4. Survivor formation in *cdc13-4* and *est2*Δ mutants. Southern blot of *Xho*I-digested genomic yeast DNA probed with a poly(GT)$_{20}$ oligonucleotide specific for telomeric repeats is shown. The bracket indicates the telomeric GT repeat band derived from Y′ element-containing chromosomes. Asterisks indicate terminal fragments derived from non-Y′ element-containing chromosomes. The arrows indicate restriction fragments corresponding to the subtelomeric Y′ elements. After tetrad dissection, spores W303 *cdc13-4* and W303 *est2*Δ from one tetrad were grown for 150 generations as described in Materials and Methods. Lane 1, W303a wild type (wt); lane 2, *est2*Δ, 25 generations; lane 3, *est2*Δ, 50 generations; lane 4, *est2*Δ, 75 generations; lane 5, *est2*Δ, 100 generations; lane 6, *est2*Δ, 125 generations; lane 7, *cdc13-4*, 25 generations; lane 8, *cdc13-4*, 50 generations; lane 9, *cdc13-4*, 75 generations; lane 10, *cdc13-4*, 100 generations; lane 11, *cdc13-4*, 125 generations.

meric GT repeat tracts after approximately 50 generations (Fig. 2, lane 1). After 150 generations (Fig. 2, lane 3), telomeric GT repeat tracts were almost as short as those observed for *yku70*-deficient strains (Fig. 2, lane 9). However, no further telomere shortening was observed after an additional 100 generations (Fig. 2, lane 5) and after several hundred generations (data not shown). Introduction of the *cdc13-4* mutation in a CEN.PK2 genetic background resulted in a comparable telomere length phenotype (data not shown).

***cdc13-4* mutants display no senescence phenotype.** Telomerase deficiency results in replicative senescence. Telomeres shorten gradually with increasing generations, eventually leading to cell death (28, 34). However, a few survivors can arise in a senescent yeast culture. These survivors stabilize their telomeres by homologous recombination, adding Y′ elements or GT repeats to the shortened chromosome ends (33). This process is detectable by an increase in intensity of the Y′ element signals in a Southern blot. Deletion of *RAD52* completely abolishes homologous recombination, and therefore no survivors appear in an *est2*/*rad52*-negative strain (27). To verify the observation that *cdc13-4* mutant cells display shortened telomeres but no senescence phenotype, we generated the diploid strain BMY58, heterozygous for *est2*Δ and *cdc13-4* mutation. After sporulation we compared growth of an *est2*Δ spore and a *cdc13-4* mutant spore (Fig. 3).

Whereas *est2*-negative cells displayed a significant growth reduction after 50 generations and survivor formation occurred after 75 generations, *cdc13-4* mutant cells grew normally over the entire time frame tested (Fig. 3). We analyzed telomere repeat sequences in BMY59-6C (*est2*Δ) and BMY59-6B (*cdc13-4*) cells by Southern blotting after growth for 25, 50, 75, 100, and 125 generations (Fig. 4).

As expected, telomeric GT repeat tracts shortened dramatically in an *est2*Δ mutant within 50 generations (Fig. 4, lanes 2 and 3). Survivor formation became obvious by the appearance of randomly sized telomeric fragments after 75 generations and the significant amplification of Y′ elements after 100 and 125 generations (Fig. 4, lanes 4 to 6). In contrast, the rate of GT repeat shortening was clearly reduced in a *cdc13-4* mutant (Fig. 4, lanes 7 to 11) compared to *est2*Δ cells and telomeres

did not reach the critical length where Y′ element amplification starts in *est2*Δ strains. We observed no increase in Y′ element signals in BMY59-6B cells after growth for 125 generations (Fig. 4, lane 11) or 250 generations (Fig. 2, lane 5). Furthermore, a *cdc13-4*/*rad52* double mutant, BMY18, displayed no growth reduction after several hundred generations (data not shown). Telomeres were as short as those observed for the single *cdc13-4* mutant and stayed stable at this short level (data not shown).

To investigate whether the rate of telomere shortening is increased in a *cdc13-4*/*est2* double mutant, we compared the growth behavior of an *est2*Δ spore and a *cdc13-4*/*est2*Δ spore from a tetrad of strain BMY58. The double mutant displayed significant growth reduction after 50 generations and survivor formation after 75 generations comparable to that of the *est2*Δ single mutant (Fig. 3). In addition, telomere shortening was not accelerated and Y′ element amplification occurred in both strains after 75 generations (data not shown).

Cdc13p and Tel1p function in different pathways of telomere length maintenance. The synthetic lethality of the *cdc13-4* mutation with a *yku70* or *yku80* deletion indicates that Cdc13p and the Yku heterodimer have independent but in some way overlapping functions at the telomere. Along with the Yku heterodimer and Cdc13p, a pathway comprised of Tel1p and the Mre11p-Xrs2p-Rad50p complex is involved in telomere length maintenance (47). To investigate if *CDC13* is epistatic to *TEL1* we generated the diploid strain BMY57, heterozygous for *tel1*Δ and *cdc13-4*. Telomeres of BMY57 cells were shorter than those of the diploid wild type (Fig. 5, compare lanes 1 and 2), indicating that reduced protein levels in the heterozygous strain already influence telomere length maintenance. For further analysis we used all four spores derived from a tetratype tetrad.

As shown in Fig. 5, the rate of GT repeat loss was accelerated in *tel1*Δ cells (Fig. 5, lane 3) compared to that in *cdc13-4* mutant cells (Fig. 5, lane 6). At the steady-state level, telomeres of *tel1*Δ cells were significantly shorter than those of *cdc13-4* mutant cells (Fig. 5, lanes 4, 5, 7, and 8). The rate of telomere shortening in the *cdc13-4*/*tel1*Δ double mutant strain (Fig. 5, lane 9) seemed not to be accelerated compared to that in *tel1*Δ (Fig. 5, lane 3), but the telomeres of the double mutant were shorter than the telomeres of either single mutant after 125 generations (Fig. 5, lanes 4, 7, and 10). After 225 generations we observed a dramatic increase in Y′ element signals in the *cdc13-4*/*tel1*Δ double mutant (Fig. 5, lane 11), indicating that telomeres were stabilized by Y′ element amplification. Although the growth of *cdc13-4*/*tel1*Δ mutants seemed to be reduced after 100 generations, cells did not cease growth completely and no fast-growing survivors occurred. Instead, colonies of the double mutant formed during a further 100 generations of growth were significantly smaller than those of either single mutant or wild type (data not shown).

Cdc13-4p is not altered in its binding to Est1p. Expression of a Cdc13-Est1 fusion protein complements a *cdc13* or *est1* deletion and, moreover, results in a dramatic increase in telomere length (12). These data suggest that the telomere-bound Cdc13p recruits telomerase via interaction with Est1p to the ssDNA overhang at chromosome ends. To examine if a reduced association with Est1 causes the telomere shortening phenotype of a *cdc13-4* mutant, we analyzed the effect of expressing a Cdc13-4–Est1 fusion on telomere length. Therefore, a Cdc13-Est1 or Cdc13-4–Est1 fusion protein was expressed under the control of the CDC13 promoter from a single-copy plasmid in wild-type, *cdc13-4*, and *cdc13*Δ cells.

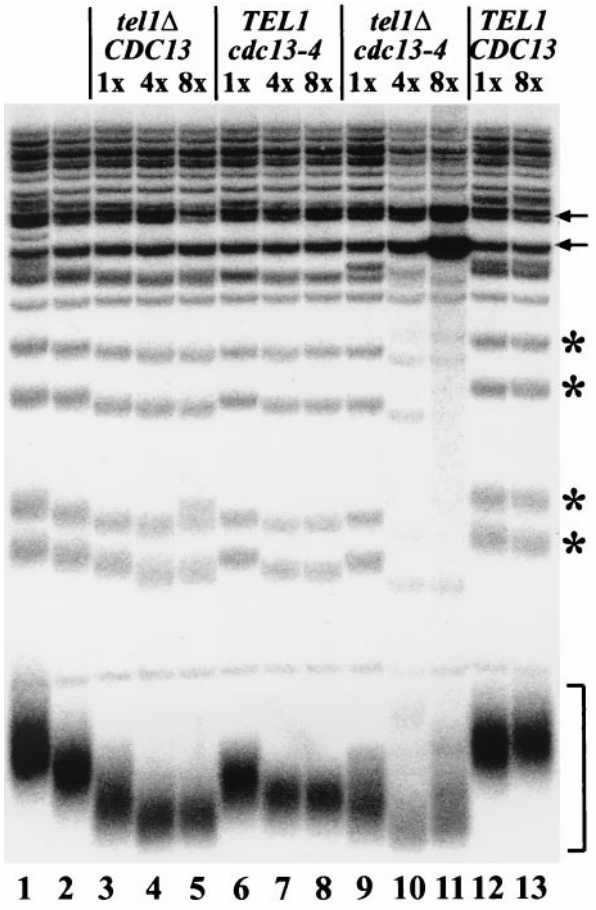

FIG. 5. Telomere length of *cdc13-4, tel1*Δ, and *cdc13-4*/*tel1*Δ mutants. Southern blot of genomic yeast DNA, probed with a telomere-specific poly$(GT)_{20}$ oligonucleotide, is shown. Spores from a tetratype tetrad of BMY57 were propagated for 225 generations as described in Materials and Methods. The bracket indicates the telomeric GT repeat band derived from Y′ element-containing chromosomes. Asterisks indicate terminal fragments derived from non-Y′ element-containing chromosomes. The arrows indicate restriction fragments corresponding to the subtelomeric Y′ elements. Lane 1, W303aα wild type; lane 2, W303aα *cdc13-4*/CDC13 *tel1*Δ/TEL1 (BMY57); lane 3, W303α *tel1*Δ, 50 generations; lane 4, W303α *tel1*Δ, 125 generations; lane 5, W303α *tel1*Δ, 225 generations; lane 6, W303a *cdc13-4*, 50 generations; lane 7, W303a *cdc13-4*, 125 generations; lane 8, W303a *cdc13-4*, 225 generations; lane 9, W303α *tel1*Δ/*cdc13-4*, 50 generations; lane 10, W303α *tel1*Δ/*cdc13-4*, 125 generations; lane 11, W303α *tel1*Δ/*cdc13-4*, 225 generations; lane 12, W303a wild type, 50 generations; lane 13, W303a wild type, 225 generations.

Expression of either fusion protein resulted in significant telomere elongation in wild-type and *cdc13-4* strains (Fig. 6A). We observed no differences in telomere elongation between mutant Cdc13-4–Est1p- and wild-type Cdc13-Est1p-expressing cells (Fig. 6A, lanes 2, 3, 5, and 6), indicating that both proteins bind with comparable affinities to chromosome ends. The effects of the fusion proteins on telomere length were not as pronounced as expected, and although the expression of the

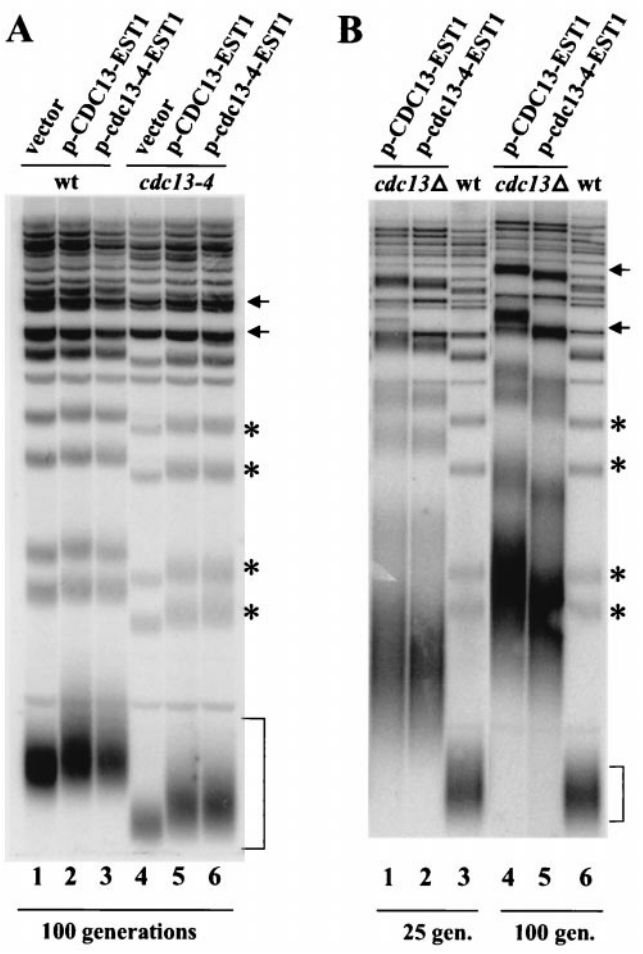

FIG. 6. Influence of Cdc13-Est1 and Cdc13-4–Est1 fusion proteins on telomere length. (A) Southern blot of W303a wild-type (wt) and W303a *cdc13-4* strains transformed with plasmids pRS316, p-CDC13-EST1, and p-cdc13-4-EST1 probed with a poly$(GT)_{20}$ oligonucleotide. Transformants were cultured for 100 generations on selective media prior to DNA preparation. Lane 1, W303a wt + pRS316 control; lane 2, W303a wt + p-CDC13-EST1; lane 3, W303a wt + p-cdc13-4-EST1; lane 4, W303a *cdc13-4* + pRS316 control; lane 5, W303a *cdc13-4* + p-CDC13-EST1; lane 6, W303a *cdc13-4* + p-cdc13-4-EST1. (B) Southern blot of W303a *cdc13*Δ strains transformed with plasmids p-CDC13-EST1 and p-cdc13-4-EST1 probed with a poly$(GT)_{20}$ oligonucleotide. Transformants were cultured for 25 or 100 generations prior to DNA preparation.

Cdc13-Est1 fusion protein in *cdc13-4* cells leads to GT tract elongation, the telomeres of these cells did not reach wild-type level. These results point toward a competition between the fusion protein and cellularly expressed Cdc13p alleles. When the influence of the fusion proteins on telomere maintenance was examined in a *cdc13*Δ strain, dramatically elongated telomeric GT repeat tracts were observed after 100 generations. However, the Cdc13-4–Est1 fusion protein (Fig. 6B, lane 5) did not induce telomere elongation to the same extent as a Cdc13-Est1 fusion (Fig. 6B, lane 4). These data suggest that the Cdc13-4–Est1 fusion is capable of binding the telomeric ends and provokes deregulated telomere elongation. Hence, since the Cdc13-4–Est1 fusion does not lead to telomere elongation as observed for Cdc13-Est1p, the establishment of a permanent interaction between Cdc13-4p and Est1p, thereby tethering telomerase to the telomere, seems not sufficient to complement the *cdc13-4* mutation.

To verify that the Cdc13p-Est1p interaction is not altered in a *cdc13-4* mutant, we performed coimmunoprecipitation experiments. Recently it was reported (45) that a Cdc13-Est1 interaction can be detected biochemically if both proteins are overexpressed. Therefore, we generated strains expressing the chromosomal copy of *CDC13* or *cdc13-4* as an N-terminal HA_3-tagged protein and Est1p as a GST fusion protein under control of the inducible, strong *GAL1* promoter. Anti-GST monoclonal antibodies were used to precipitate GST-Est1 fusion proteins, and precipitates were analyzed by Western blotting for HA_3-Cdc13p or HA_3-Cdc13-4p.

Although only a small portion of the GST-Est1 fusion protein interacts with Cdc13p, no differences in the amount of coimmunoprecipitated HA_3-Cdc13p (Fig. 7, lane 9) or HA_3-Cdc13-4p (Fig. 7, lanes 6 and 10) protein were detectable. We did not observe cross-reaction of HA_3-Cdc13p with the anti-GST antibody (Fig. 7, lane 8), and no signal was detectable when GST-Est1p was immunoprecipitated from extracts containing wild-type Cdc13 without the HA tag (Fig. 7, lane 7). From these data we conclude that the Cdc13-4 mutant protein is not altered in its ability to interact with Est1p.

***cdc13-4* mutation seems not to affect DNA binding.** Very recently, different mutant alleles of *CDC13* that cause stably shortened telomeres comparable to the *cdc13-4* mutation have been described. These mutant Cdc13 proteins seem to display significantly reduced binding activity to telomeric DNA (18). Although expression of Cdc13-Est1p in *cdc13-4* cells indicates that Cdc13-4p and Cdc13p compete for telomere binding, we wanted to determine if the DNA binding activity of Cdc13-4p is reduced compared to that of wild-type Cdc13p. Assuming that overexpression of Cdc13-4p should complement a reduced DNA binding activity, we analyzed telomere length in the diploid strain HFY82 expressing one wild-type copy of *CDC13* and one copy of HA_3-*cdc13-4* under control of the inducible *GAL1* promoter.

After growth on glucose-containing media, the telomere length of HFY82 cells was comparable to that of wild type (Fig. 8, lanes 1 and 4), indicating that one wild-type copy of *CDC13* was sufficient for telomere stability. Strikingly, after growth under inducing conditions on galactose for approximately 50 generations, telomeres were significantly shorter than those of the wild type (Fig. 8, lane 5). Telomere shortening was already obvious in the heterozygous strain BMY56, where Cdc13p and Cdc13-4p were expressed from the native *CDC13* promoter (Fig. 8, lane 3), even though GT repeat tract loss was not as pronounced as seen in a haploid *cdc13-4* mutant (Fig. 8, lane 2). In addition, cooverexpression of HA_3-Cdc13-4p and GST-Est1p could not restore wild-type telomere length, but it did induce telomere shortening (Fig. 8, lane 7). Therefore, Cdc13-4p is at least in part dominant on Cdc13p and might compete with Cdc13p for telomere binding. These data indicate that neither DNA binding activity nor interaction with Est1 is reduced in a Cdc13-4 mutant protein.

It has been proposed that Ccd13p protects chromosome ends from degradation by binding to the ss 3′ GT overhang. At the restrictive temperature, *cdc13-1*^{ts} cells exhibit an increased amount of ssDNA in telomeric and subtelomeric regions (16).

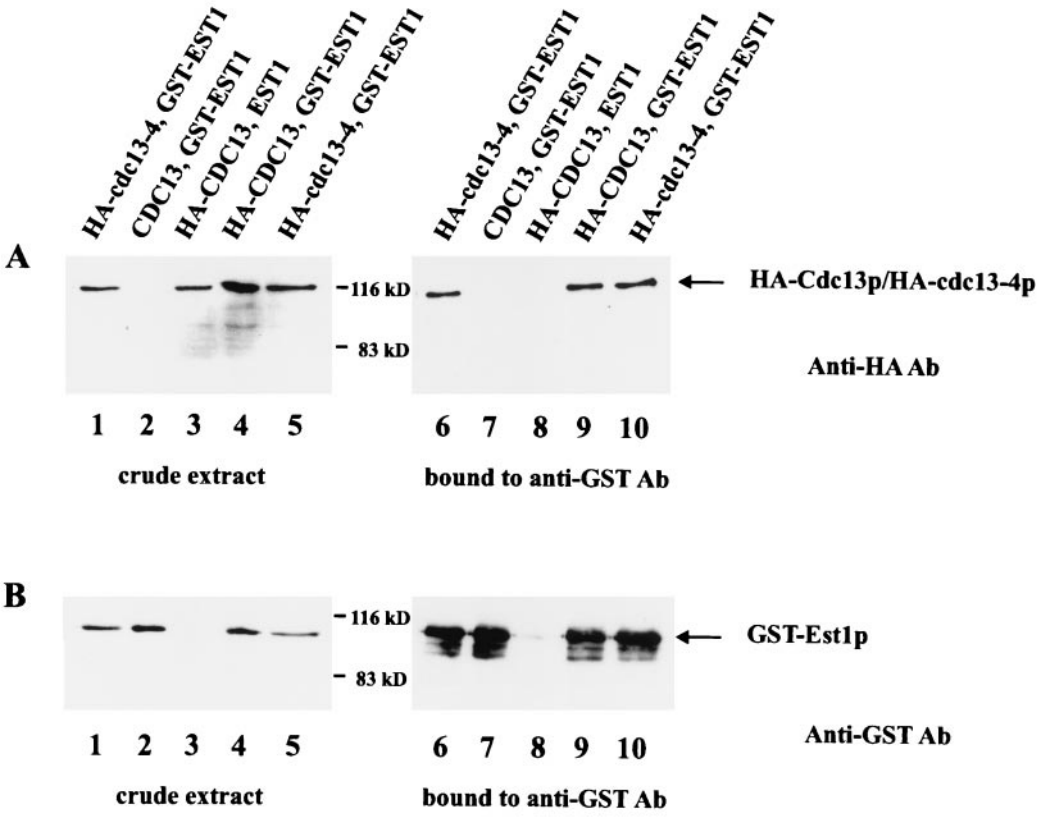

FIG. 7. Coimmunoprecipitation of HA-*cdc13-4* with GST-Est1. Ten-microgram samples of crude extracts were loaded to compare the protein amounts of different mutants used for coimmunoprecipitation experiments (lanes 1 to 5). Coimmunoprecipitation of Cdc13p and Est1p was performed as described in Materials and Methods (lanes 6 to 10). Crude extract (1,000 μg) was incubated with 5 μg of anti-GST antibody, and G-Sepharose beads were used to isolate antibody and bound proteins. After intensive washing, G-Sepharose beads were heated to 95°C in Laemmli buffer and the supernatant was loaded onto an 8% sodium dodecyl sulfate gel. (A) Lane 1, HFY86-3A (HA-cdc13-4p, GST-Est1p); lane 2, HFY81-8A (Cdc13p, GST-Est1p); lane 3, HFY82-6B (HA-Cdc13p, Est1p); lane 4, HFY82-4C (HA-Cdc13p, GST-Est1p); lane 5, HFY86-9D (HA-cdc13-4p, GST-Est1p); lane 6, HFY86-3A (HA-cdc13-4, GST-EST1); lane 7, HFY81-8A (Cdc13p, GST-Est1p); lane 8, HFY82-6B (HA-Cdc13p, Est1p); lane 9, HFY82-4C (HA-Cdc13p, GST-Est1p); lane 10, HFY86-9D (HA-cdc13-4p, GST-Est1p). HA-Cdc13p and HA-Cdc13-4p were detected by anti-HA antibody. (B) The same blots as in panel A probed with an anti-GST antibody. Note that lanes 6 to 10 were exposed a significantly shorter time to detect the GST-Est1p signals than lanes 1 to 5 and blots probed with anti-HA antibody in panel A. Ab, antibody.

To investigate whether a *cdc13-4* mutant displays an accumulation of ssDNA at the telomeres, we performed nondenaturing in-gel hybridization using a synthetic oligonucleotide specific for telomeric GT repeats. As a control we used *yku80* mutant cells that have been shown to contain a long ss overhang of the G-rich strand throughout the cell cycle (19).

In contrast to *yku80* mutants, the ssDNA signal of the *cdc13-4* mutant remained at a wild-type level after growth for 40 (Fig. 9, lanes 2 and 4) and 260 (Fig. 9, lanes 3 and 5), generations. Therefore, chromosome ends still seem to be protected from nucleolytic degradation by the Cdc13-4 mutant protein.

DISCUSSION

S. cerevisiae CDC13 is an essential gene involved in chromosome end replication and protection. The *cdc13-4* allele, which we isolated in a synthetic lethality screen with *YKU70*, causes a dramatic shortening of GT repeats at the telomeres but the strain remains viable. Telomere shortening proceeds slowly over approximately 150 generations; however, telomere length is stabilized at a short level after 200 generations (Fig. 2). This telomere phenotype is distinct from the senescence phenotype of a *cdc13-2^{est}* allele, which leads to progressive telomere shortening and eventually cell death (40). In a senescent yeast culture a few cells occasionally escape from cell death. These survivors stabilize their telomeres by adding either tandem copies of the subtelomeric Y′ elements or $C_{1-3}A/TG_{1-3}$ repeats in a *RAD52*-dependent recombination process (53). *cdc13-4* mutants do not display Y′ element amplification in a Southern blot as observed in survivors of telomerase-negative yeast strains (Fig. 2 and 4). In addition, a *cdc13-4*/*rad52* double mutant strain is viable for more than 250 generations while maintaining short telomeres (data not shown). Therefore, *cdc13-4* mutants do not show characteristics of a senescent mutant and telomeres do not reach the critical length level which triggers telomere stabilization by homologous recombination. Compared to that of an *est2*Δ mutant, the rate of telomere shortening in a *cdc13-4* mutant is clearly reduced (Fig. 4), indicating that telomerase activity is altered but not abolished. The stabilization of telomere length at a shorter level shows that telomerase is fully active at the new equilibrium length.

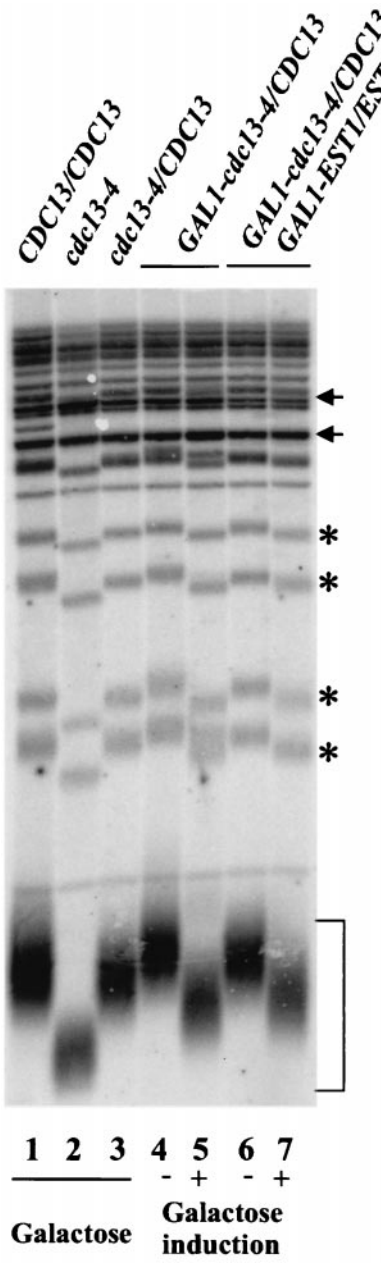

FIG. 8. Overexpression of *cdc13-4* in a heterozygous mutant strain. Diploid strains W303aα, BMY56 (*cdc13-4*/CDC13), and BMY17 (*cdc13-4*) were grown on galactose-containing media, whereas HFY84 (*GAL1-cdc13-4*/CDC13) and HFY86 (*GAL1-cdc13-4*/CDC13 *GAL1*-EST1/EST1) were simultaneously grown under inducing and noninducing conditions. Telomere length was investigated after 50 generations. Lane 1, W303aα; lane 2, BMY17 (*cdc13-4*); lane 3, BMY56 (*cdc13-4*/CDC13); lane 4, HFY84 (*GAL1-cdc13-4*/CDC13) grown on glucose; lane 5, HFY84 (*GAL1-cdc13-4*/CDC13) grown on galactose; lane 6, HFY86 (*GAL1-cdc13-4*/CDC13 *GAL1*-EST1/EST1) grown on glucose; lane 7, HFY86 (*GAL1-cdc13-4*/CDC13 *GAL1*-EST1/EST1) grown on galactose. Brackets indicate terminal GT repeats, asterisks indicate non-Y′ elements, and the arrows represent Y′ element bands.

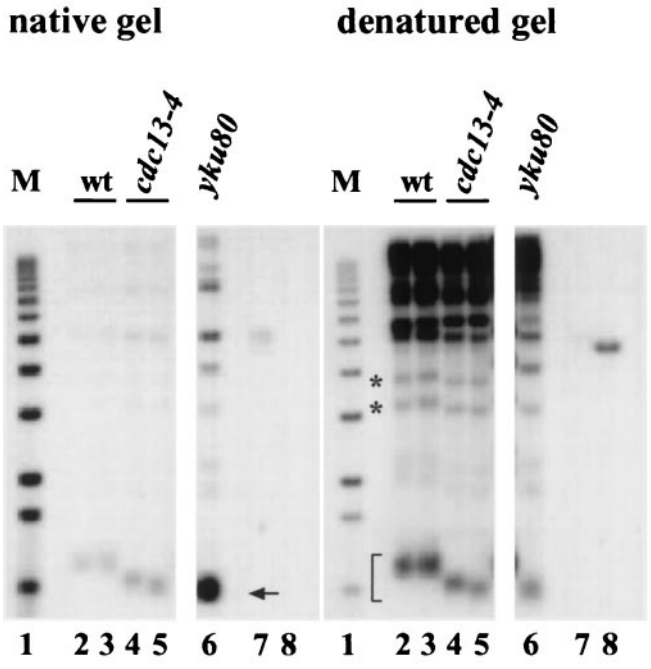

FIG. 9. Telomeric end structure in *cdc13-4* mutant cells. W303 wild-type (wt) and W303 *cdc13-4* spores derived from one tetrad were streaked on YPD for 250 generations and used for genomic DNA preparation as described in Materials and Methods. (Left panel) After *Xho*I digestion, genomic DNA was separated by gel electrophoresis and analyzed by nondenaturing in-gel hybridization using a 22-mer $C_{1-3}A$ oligonucleotide as a probe. The arrow indicates terminal restriction fragments derived from Y′ element-containing chromosomes. The strong signal in lane 6 corresponds to the elongated ssDNA overhang in *yku80*-deficient cells. Lane 1, 1-kbp ladder DNA; lane 2, W303 wt, 40 generations; lane 3, W303 wt, 260 generations; lane 4, W303 *cdc13-4*, 40 generations; lane 5, W303 *cdc13-4*, 260 generations; lane 6, *yku80* mutant; lane 7, control ssDNA; lane 8, control double-stranded DNA. (Right panel) The same gel as in the left panel, after denaturation of the DNA in the gel and rehybridization to the same probe. The bracket indicates the telomeric GT repeat band derived from Y′ element-containing chromosomes. Asterisks indicate terminal fragments derived from non-Y′ element-containing chromosomes.

Mutations in *TEL1* and *TEL2* have been reported to cause a progressive telomere shortening phenotype comparable to that of *cdc13-4*. Telomeres in *tel1-1* and *tel2-1* mutants shorten to a stable level within 150 generations (35, 48), and a *tel1-1*/*tel2-1* double mutant has no telomeres shorter than those of *tel1-1* cells. This suggests that Tel1p and Tel2p function in the same pathway of telomere maintenance (25, 35). In contrast, a *cdc13-4*/*tel1*Δ double mutant displays slightly shorter GT repeat tracts after 125 generations compared to those of a *tel1*Δ or a *cdc13-4* single mutant. In addition, Y′ elements are amplified in the double mutant after 225 generations (Fig. 5), indicating that telomeres have shortened to a critical level. These data point toward a function of *CDC13* in telomere maintenance independent of the *TEL1* pathway.

The *cdc13-4* mutation is synthetically lethal with *yku70* or *yku80* (Fig. 1). This might be explained by a reduced telomere capping ability of the Cdc13-4 protein, which becomes essential at the elongated ssDNA overhang in Yku$^-$ mutants (19). This would then lead to the degradation of chromosome ends and cell cycle arrest. However, our data do not support such a model. Formation of microcolonies from double mutant spores (Fig. 1) makes it more likely that accelerated senescence is the reason for the synthetic lethality. Telomeres in Yku$^-$ mutants are shortened severely, and any further GT repeat tract short-

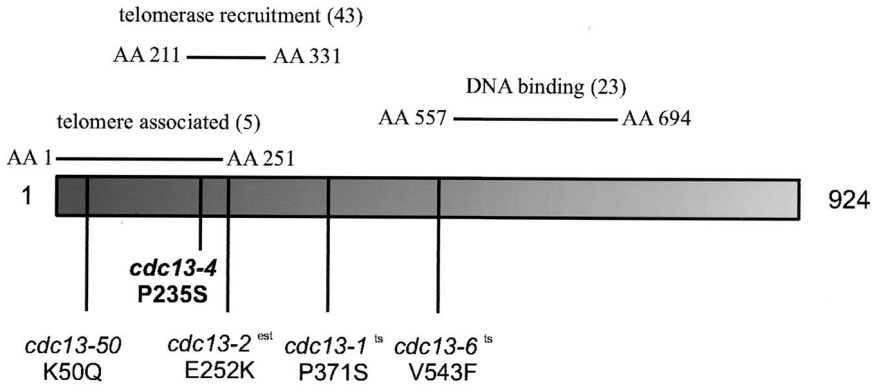

	mutation	phenotype	reference
cdc13-1	P371S	temperature-sensitive	(40)
cdc13-2	E252K	progressive telomere shortening, senescence	(40)
cdc13-3	n.d.	telomere elongation	(41)
cdc13-6	V543F	temperature-sensitive	(23)
cdc13-50	K50Q	telomere elongation	(45)
cdc13-69	n.d.	stably shortened telomeres	(18)
cdc13-109	n.d.	telomere elongation	(18)
cdc13-4	P235S	stably shortened telomeres	this study

FIG. 10. Functional domains and selected mutations of *CDC13* mutants. AA, amino acid; n.d., not determined.

ening by the *cdc13-4* mutation would result in reaching a lethal level within a few generations.

Cdc13p has been proposed to control the susceptibility of chromosome ends to the specific degradation of the telomeric $C_{1-3}A$ strand at the end of S phase (57), and therefore a reduced DNA binding activity of Cdc13-4p could possibly cause a progressive telomere shortening as seen in *cdc13-4* cells. The *cdc13-4* mutation at position 235 is not located in the DNA binding domain of Cdc13p (23) (Fig. 10), although this does not exclude a conformational change in the Cdc13-4 mutant protein resulting in reduced DNA binding activity. Cdc13p protects chromosome ends from degradation and thereby prevents the generation of telomeric ssDNA (16, 40). Therefore we would expect at least a slight increase in ssDNA at the telomeres in *cdc13-4* cells if Cdc13-4p is reduced in DNA binding. However, native in-gel hybridization experiments revealed no increase in ssDNA formation in *cdc13-4* mutants (Fig. 9).

The expression of a Cdc13-Est1 or Cdc13-Est2 fusion protein in *cdc13*Δ strains has been shown to complement for telomerase deficiency and additionally results in strongly elongated telomeres. Therefore, the expression of a mutant Cdc13-4–Est1 fusion protein should exhibit telomere elongation comparable to that of a wild-type Cdc13-Est1 fusion protein if DNA binding of Cdc13-4p is not reduced. In fact, telomere elongation was detected in strains expressing the mutant Cdc13-4–Est1 or the wild-type Cdc13-Est1 fusion protein (Fig. 6). Furthermore, GT repeat tract length in *cdc13-4* cells expressing the wild-type Cdc13-Est1 fusion protein, although significantly elongated, did not reach the wild-type level after 100 generations (Fig. 6B), suggesting that endogenous Cdc13-4p can compete with the Cdc13-Est1 fusion protein for telomere binding, thereby partially preventing telomere elongation.

Additional evidence that DNA binding is unchanged is provided by the finding that heterozygous *CDC13*/*cdc13-4* diploid yeast strains show reduced telomere length (Fig. 8), indicating an at least partially dominant phenotype of the *cdc13-4* mutation. Telomere shortening in the heterozygous *CDC13*/*cdc13-4* diploid strains is not caused by a reduced amount of functional Cdc13p since a *CDC13*/*GAL1*-HA_3-*cdc13-4* strain exhibits wild-type telomere length (Fig. 8) on glucose where expression of HA_3-*cdc13-4* by the *GAL1* promoter is repressed. The dominant phenotype of Cdc13-4p is even more pronounced if overexpression of HA_3-*cdc13-4* is induced in the heterozygous diploid (Fig. 8). This again indicates that Cdc13-4p competes with wild-type Cdc13p for telomere binding. Therefore, we present evidence that the mutant Cdc13-4 protein is capable of chromosome end binding with an affinity comparable to that of the wild-type Cdc13p. An alternative explanation for the partially dominant phenotype of the *cdc13-4* mutation would be a competition of wild-type Cdc13p and mutant Cdc13-4p for a protein important for telomere elongation. Further experiments have to be performed to address this question.

The recruitment of telomerase to chromosome ends seems to take place via the interaction of Cdc13p and Est1p. Therefore, an attenuated interaction of Cdc13-4p and Est1p could

cause telomere shortening to a stable level. The telomerase recruitment site of Cdc13p was recently mapped to amino acids 211 to 331 (43). The *cdc13-4* mutation (P235S) is located near the border of this domain; thus, the interaction of the mutant Cdc13-4 protein and Est1p might be reduced. Nevertheless, we found no reduced interaction of Cdc13-4p–Est1p in coimmunoprecipitation experiments (Fig. 7). In addition, overexpression of Cdc13-4p or cooverexpression of Cdc13-4p and Est1p induces telomere shortening in a heterozygous diploid strain (Fig. 8) and did not complement the *cdc13-4* mutation as we would suggest for a weakened interaction.

Significantly elongated telomeres, most likely the result of unregulated access of the active telomerase complex to the telomere, are detectable in yeast strains expressing a Cdc13-Est1 fusion protein (12). Although the Cdc13-4–Est1 fusion protein causes a dramatic telomere elongation in a *cdc13*Δ strain, the effect is not as pronounced as that observed for a wild-type Cdc13-Est1 fusion. Therefore, establishing a permanent interaction of Cdc13-4p and Est1p is not sufficient to complement the *cdc13-4* mutation to wild-type level, indicating that a function independent of interaction with Est1p is affected in Cdc13-4p. The DNA binding domain of Cdc13p has been mapped to an internal part of the protein (23); nevertheless, the N-terminal 251 amino acids of Cdc13p associate in vivo with the telomere (5), indicating tight interaction with telomere bound proteins. This N-terminal domain partially overlaps the telomerase recruiting domain of Cdc13p (43) (Fig. 10) but seems not to be sufficient for Cdc13p-Est1p interaction. Thus, the *cdc13-4* mutation might influence interaction with other proteins at the telomere, thereby preventing appropriate activation of telomerase activity.

In *S. cerevisiae*, telomere length seems to be maintained by the balance of two antagonistic processes—telomere elongation and telomere shortening. Many proteins are necessary to maintain normal telomere length. Deletion of one Yku subunit (3, 44) or inactivation of a member of the *TEL1* pathway, comprised of Tel1p, Mre11p, Xrs2p, and Rad50p, leads to telomere shortening to a stable level (2, 20). The additional telomere shortening seen in *yku70*/*tel1* or *yku70*/*rad50* double mutants indicates that the Yku heterodimer has a *TEL1*-independent role in telomere maintenance (47). In *cdc13-4* mutant cells, telomerase seems to be inactive at normal telomere length, indicating that Cdc13p is involved in positive telomere length regulation by activating telomerase at short GT repeat levels. The further telomere shortening seen in *cdc13-4*/*tel1*Δ double mutants and the synthetic lethality of *cdc13-4* with a Yku subunit deletion lead to the conclusion that at least three independent pathways are involved in positive telomere length regulation and that Ccd13p is an essential part of one of these pathways.

However, the addition of telomeric GT repeats to telomeric ends depends not only on telomerase but also on DNA polymerases Pol α, Pol δ, and DNA primase, most likely by a coordinated regulation of C- and G-strand synthesis (10). Recently it has been shown that Cdc13p interacts with Pol1p, the catalytic subunit of DNA polymerase α. Single point mutations in either *CDC13* or *POL1* that weaken the interaction of Cdc13p with Pol1p result in telomerase-dependent telomere lengthening (45). Therefore Cdc13p also seems to play an important role in negative telomere length control, presumably by coordinating telomeric C- and G-strand synthesis.

Until now three different functions of Cdc13p in telomere maintenance have been defined by *CDC13* mutations (Fig. 10): (i) protection of chromosome ends from nucleolytic degradation (abolished in a *cdc13-1*^{ts} mutant at the restrictive temperature), (ii) loading of telomerase onto the ssDNA overhang at the telomere (prevented in *cdc13-2*^{est} cells), and (iii) regulation of telomere length. The role of Cdc13p in telomere length control seems to be multifaceted, since mutating *CDC13* can cause either telomere lengthening, seen in *cdc13-50* mutants (45) and different mutant *CDC13* alleles (18), or telomere shortening to a new steady-state level, seen in newly identified *CDC13* mutants (18) and the *cdc13-4* mutant reported here. Our data present evidence that Cdc13p plays a key role not only in recruiting telomerase but also in modulating its access to the telomere, which might be influenced by additional regulatory proteins.

ACKNOWLEDGMENTS

We thank E. Schiebel for yeast strains and plasmids. We are grateful to R. J. Wellinger for ssDNA analysis. We also thank S. Eimer for helpful discussions during this project and S. Eimer and B. Lakowski for valuable comments on the manuscript.

B. Meier and L. Driller contributed equally to the work.

This work was supported by Deutsche Forschungsgemeinschaft grant Wi 319/11-3, Project 7.

REFERENCES

1. **Bojunga, N., P. Kotter, and K. D. Entian.** 1998. The succinate/fumarate transporter Acr1p of *Saccharomyces cerevisiae* is part of the gluconeogenic pathway and its expression is regulated by Cat8p. Mol. Gen. Genet. **260:** 453–461.
2. **Boulton, S. J., and S. P. Jackson.** 1998. Components of the Ku-dependent non-homologous end-joining pathway are involved in telomeric length maintenance and telomeric silencing. EMBO J. **17:**1819–1828.
3. **Boulton, S. J., and S. P. Jackson.** 1996. Identification of a *Saccharomyces cerevisiae* Ku80 homologue: roles in DNA double strand break rejoining and in telomeric maintenance. Nucleic Acids Res. **24:**4639–4648.
4. **Boulton, S. J., and S. P. Jackson.** 1996. *Saccharomyces cerevisiae* Ku70 potentiates illegitimate DNA double-strand break repair and serves as a barrier to error-prone DNA repair pathways. EMBO J. **15:**5093–5103.
5. **Bourns, B. D., M. K. Alexander, A. M. Smith, and V. A. Zakian.** 1998. Sir proteins, Rif proteins, and Cdc13p bind *Saccharomyces* telomeres in vivo. Mol. Cell. Biol. **18:**5600–5608.
6. **Cohn, M., and E. H. Blackburn.** 1995. Telomerase in yeast. Science **269:** 396–400.
7. **Conrad, M. N., J. H. Wright, A. J. Wolf, and V. A. Zakian.** 1990. RAP1 protein interacts with yeast telomeres in vivo: overproduction alters telomere structure and decreases chromosome stability. Cell **63:**739–750.
8. **Counter, C. M., M. Meyerson, E. N. Eaton, and R. A. Weinberg.** 1997. The catalytic subunit of yeast telomerase. Proc. Natl. Acad. Sci. USA **94:**9202–9207.
9. **Cvrckova, F., and K. Nasmyth.** 1993. Yeast G1 cyclins CLN1 and CLN2 and a GAP-like protein have a role in bud formation. EMBO J. **12:**5277–5286.
10. **Diede, S. J., and D. E. Gottschling.** 1999. Telomerase-mediated telomere addition in vivo requires DNA primase and DNA polymerases alpha and delta. Cell **99:**723–733.
11. **Dionne, I., and R. J. Wellinger.** 1996. Cell cycle-regulated generation of single-stranded G-rich DNA in the absence of telomerase. Proc. Natl. Acad. Sci. USA **93:**13902–13907.
12. **Evans, S. K., and V. Lundblad.** 1999. Est1 and Cdc13 as comediators of telomerase access. Science **286:**117–120.
13. **Fan, H. Y., K. K. Cheng, and H. L. Klein.** 1996. Mutations in the RNA polymerase II transcription machinery suppress the hyperrecombination mutant hpr1 delta of *Saccharomyces cerevisiae*. Genetics **142:**749–759.
14. **Feldmann, H., L. Driller, B. Meier, G. Mages, J. Kellermann, and E. L. Winnacker.** 1996. HDF2, the second subunit of the Ku homologue from *Saccharomyces cerevisiae*. J. Biol. Chem. **271:**27765–27769.
15. **Feldmann, H., and E. L. Winnacker.** 1993. A putative homologue of the human autoantigen Ku from *Saccharomyces cerevisiae*. J. Biol. Chem. **268:** 12895–12900.
16. **Garvik, B., M. Carson, and L. Hartwell.** 1995. Single-stranded DNA arising

at telomeres in *cdc13* mutants may constitute a specific signal for the *RAD9* checkpoint. Mol. Cell. Biol. **15:**6128–6138. (Erratum, **16:**457, 1996.)
17. **Geissler, S., K. Siegers, and E. Schiebel.** 1998. A novel protein complex promoting formation of functional alpha- and gamma-tubulin. EMBO J. **17:**952–966.
18. **Grandin, N., C. Damon, and M. Charbonneau.** 2000. Cdc13 cooperates with the yeast Ku proteins and Stn1 to regulate telomerase recruitment. Mol. Cell. Biol. **20:**8397–8408.
19. **Gravel, S., M. Larrivee, P. Labrecque, and R. J. Wellinger.** 1998. Yeast Ku as a regulator of chromosomal DNA end structure. Science **280:**741–744.
20. **Greenwell, P. W., S. L. Kronmal, S. E. Porter, J. Gassenhuber, B. Obermaier, and T. D. Petes.** 1995. TEL1, a gene involved in controlling telomere length in *S. cerevisiae*, is homologous to the human ataxia telangiectasia gene. Cell **82:**823–829.
21. **Hardy, C. F., L. Sussel, and D. Shore.** 1992. A RAP1-interacting protein involved in transcriptional silencing and telomere length regulation. Genes Dev. **6:**801–814.
22. **Henderson, E. R., and E. H. Blackburn.** 1989. An overhanging 3′ terminus is a conserved feature of telomeres. Mol. Cell. Biol. **9:**345–348.
23. **Hughes, T. R., R. G. Weilbaecher, M. Walterscheid, and V. Lundblad.** 2000. Identification of the single-strand telomeric DNA binding domain of the *Saccharomyces cerevisiae* Cdc13 protein. Proc. Natl. Acad. Sci. USA **97:**6457–6462.
24. **Klobutcher, L. A., M. T. Swanton, P. Donini, and D. M. Prescott.** 1981. All gene-sized DNA molecules in four species of hypotrichs have the same terminal sequence and an unusual 3′ terminus. Proc. Natl. Acad. Sci. USA **78:**3015–3019.
25. **Kota, R. S., and K. W. Runge.** 1998. The yeast telomere length regulator TEL2 encodes a protein that binds to telomeric DNA. Nucleic Acids Res. **26:**1528–1535.
26. **Kranz, J. E., and C. Holm.** 1990. Cloning by function: an alternative approach for identifying yeast homologs of genes from other organisms. Proc. Natl. Acad. Sci. USA **87:**6629–6633.
27. **Le, S., J. K. Moore, J. E. Haber, and C. W. Greider.** 1999. RAD50 and RAD51 define two pathways that collaborate to maintain telomeres in the absence of telomerase. Genetics **152:**143–152.
28. **Lendvay, T. S., D. K. Morris, J. Sah, B. Balasubramanian, and V. Lundblad.** 1996. Senescence mutants of *Saccharomyces cerevisiae* with a defect in telomere replication identify three additional EST genes. Genetics **144:**1399–1412.
29. **Lin, J. J., and V. A. Zakian.** 1996. The *Saccharomyces* CDC13 protein is a single-strand TG1–3 telomeric DNA-binding protein in vitro that affects telomere behavior in vivo. Proc. Natl. Acad. Sci. USA **93:**13760–13765.
30. **Lingner, J., T. R. Cech, T. R. Hughes, and V. Lundblad.** 1997. Three ever shorter telomere (EST) genes are dispensable for in vitro yeast telomerase activity. Proc. Natl. Acad. Sci. USA **94:**11190–11195.
31. **Liu, C., X. Mao, and A. J. Lustig.** 1994. Mutational analysis defines a C-terminal tail domain of RAP1 essential for telomeric silencing in *Saccharomyces cerevisiae*. Genetics **138:**1025–1040.
32. **Longtine, M. S., A. McKenzie, D. J. Demarini, N. G. Shah, A. Wach, A. Brachat, P. Philippsen, and J. R. Pringle.** 1998. Additional modules for versatile and economical PCR-based gene deletion and modification in *Saccharomyces cerevisiae*. Yeast **14:**953–961.
33. **Lundblad, V., and E. H. Blackburn.** 1993. An alternative pathway for yeast telomere maintenance rescues est1$^-$ senescence. Cell **73:**347–360.
34. **Lundblad, V., and J. W. Szostak.** 1989. A mutant with a defect in telomere elongation leads to senescence in yeast. Cell **57:**633–643.
35. **Lustig, A. J., and T. D. Petes.** 1986. Identification of yeast mutants with altered telomere structure. Proc. Natl. Acad. Sci. USA **83:**1398–1402.
36. **Makarov, V. L., Y. Hirose, and J. P. Langmore.** 1997. Long G tails at both ends of human chromosomes suggest a C strand degradation mechanism for telomere shortening. Cell **88:**657–666.
37. **Marcand, S., V. Brevet, and E. Gilson.** 1999. Progressive cis-inhibition of telomerase upon telomere elongation. EMBO J. **18:**3509–3519.
38. **Marcand, S., E. Gilson, and D. Shore.** 1997. A protein-counting mechanism for telomere length regulation in yeast. Science **275:**986–990.
39. **McElligott, R., and R. J. Wellinger.** 1997. The terminal DNA structure of mammalian chromosomes. EMBO J. **16:**3705–3714.
40. **Nugent, C. I., T. R. Hughes, N. F. Lue, and V. Lundblad.** 1996. Cdc13p: a single-strand telomeric DNA-binding protein with a dual role in yeast telomere maintenance. Science **274:**249–252.
41. **Nugent, C. I., and V. Lundblad.** 1998. The telomerase reverse transcriptase: components and regulation. Genes Dev. **12:**1073–1085.
42. **Orr-Weaver, T. L., J. W. Szostak, and R. J. Rothstein.** 1983. Genetic applications of yeast transformation with linear and gapped plasmids. Methods Enzymol. **101:**228–245.
43. **Pennock, E., K. Buckley, and V. Lundblad.** 2001. Cdc13 delivers separate complexes to the telomere for end protection and replication. Cell **104:**387–396.
44. **Porter, S. E., P. W. Greenwell, K. B. Ritchie, and T. D. Petes.** 1996. The DNA-binding protein Hdf1p (a putative Ku homologue) is required for maintaining normal telomere length in *Saccharomyces cerevisiae*. Nucleic Acids Res. **24:**582–585.
45. **Qi, H., and V. A. Zakian.** 2000. The *Saccharomyces* telomere-binding protein Cdc13p interacts with both the catalytic subunit of DNA polymerase alpha and the telomerase-associated est1 protein. Genes Dev. **14:**1777–1788.
46. **Ray, A., and K. W. Runge.** 1999. The yeast telomere length counting machinery is sensitive to sequences at the telomere-nontelomere junction. Mol. Cell. Biol. **19:**31–45.
47. **Ritchie, K. B., and T. D. Petes.** 2000. The Mre11p/Rad50p/Xrs2p complex and the tel1p function in a single pathway for telomere maintenance in yeast. Genetics **155:**475–479.
48. **Runge, K. W., and V. A. Zakian.** 1996. *TEL2*, an essential gene required for telomere length regulation and telomere position effect in *Saccharomyces cerevisiae*. Mol. Cell. Biol. **16:**3094–3105.
49. **Sandell, L. L., and V. A. Zakian.** 1993. Loss of a yeast telomere: arrest, recovery, and chromosome loss. Cell **75:**729–739.
50. **Schiestl, R. H., and R. D. Gietz.** 1989. High efficiency transformation of intact yeast cells using single stranded nucleic acids as a carrier. Curr. Genet. **16:**339–346.
51. **Sikorski, R. S., and P. Hieter.** 1989. A system of shuttle vectors and yeast host strains designed for efficient manipulation of DNA in *Saccharomyces cerevisiae*. Genetics **122:**19–27.
52. **Singer, M. S., and D. E. Gottschling.** 1994. TLC1: template RNA component of *Saccharomyces cerevisiae* telomerase. Science **266:**404–409.
53. **Teng, S. C., and V. A. Zakian.** 1999. Telomere-telomere recombination is an efficient bypass pathway for telomere maintenance in *Saccharomyces cerevisiae*. Mol. Cell. Biol. **19:**8083–8093.
54. **van Steensel, B., A. Smogorzewska, and T. de Lange.** 1998. TRF2 protects human telomeres from end-to-end fusions. Cell **92:**401–413.
55. **Wach, A., A. Brachat, R. Pohlmann, and P. Philippsen.** 1994. New heterologous modules for classical or PCR-based gene disruptions in *Saccharomyces cerevisiae*. Yeast **10:**1793–1808.
56. **Weinert, T. A., and L. H. Hartwell.** 1993. Cell cycle arrest of cdc mutants and specificity of the *RAD9* checkpoint. Genetics **134:**63–80.
57. **Wellinger, R. J., K. Ethier, P. Labrecque, and V. A. Zakian.** 1996. Evidence for a new step in telomere maintenance. Cell **85:**423–433.
58. **Wellinger, R. J., A. J. Wolf, and V. A. Zakian.** 1993. *Saccharomyces* telomeres acquire single-strand TG1–3 tails late in S phase. Cell **72:**51–60.
59. **Wotton, D., and D. Shore.** 1997. A novel Rap1p-interacting factor, Rif2p, cooperates with Rif1p to regulate telomere length in *Saccharomyces cerevisiae*. Genes Dev. **11:**748–760.
60. **Wright, W. E., V. M. Tesmer, K. E. Huffman, S. D. Levene, and J. W. Shay.** 1997. Normal human chromosomes have long G-rich telomeric overhangs at one end. Genes Dev. **11:**2801–2809.